Propylene Synthesis

DOI: 10.1002/ange.201104071

Transformation of Methane to Propylene: A Two-Step Reaction Route Catalyzed by Modified CeO_2 Nanocrystals and Zeolites**

Jieli He, Ting Xu, Zhihui Wang, Qinghong Zhang, Weiping Deng, and Ye Wang**

The utilization of methane, which is the main constituent of natural gas, coal-bed gas, shale gas, and the vast gas hydrate resources, for the production of chemicals is one of the most important research targets in catalysis. The current technology for chemical utilization of methane involves high-temperature steam reforming to produce syngas, and the subsequent conversion of syngas to methanol, followed by methanol transformation. However, steam reforming of methane is an energy- and cost-intensive process. The direct transformation of methane to valuable chemicals would be the most desirable route, however, despite many efforts it remains difficult to achieve.[1] The development of novel catalytic routes for the transformation of methane is of high significance from both practical and fundamental points of view.

Monohalogenomethanes (CH_3Cl or CH_3Br) could be alternative platform molecules for the conversion of CH_4 to chemicals. Olah et al. reported the catalytic monohalogenation of CH_4 by Cl_2 or Br_2 over supported superacids or noble metals, followed by hydrolysis of methyl halides to methanol and dimethyl ether.[2] Zhou et al. disclosed the conversion of CH_4 or C_2H_6 to alkyl bromides by using Br_2, and the subsequent conversion to oxygenates through stoichiometric reactions with metal oxides.[3] GRT, Inc. developed a technology for the transformation of CH_4 to various products, particularly liquid hydrocarbon fuels, through the reaction with Br_2 via methyl bromides, and claimed that this is a cost-effective route.[4] In these processes, the generated HCl, HBr, or metal bromides must be oxidized to Cl_2 or Br_2 to complete the catalytic cycle. HBr was demonstrated to be useful for the oxidative bromination of CH_4 in the presence of O_2 instead of Br_2 over supported Ru or Rh catalysts,[5] but the high cost and limited availability of noble metals may hinder the large-scale application of this system. Zn-MCM-48-supported hydrated dibromo(dioxo)molybdenum(VI), which might generate Br_2 during reaction, catalyzed the oxidation of CH_4 to methanol and dimethyl ether, but the long-term stability of this system was not confirmed.[6] SiO_2-supported $FePO_4$ was stable for the oxidative bromination of CH_4, which provided CH_3Br with a selectivity of approximately 50%.[7] Only a few studies have been devoted to the oxidative chlorination of CH_4 to CH_3Cl, although HCl is cheaper than HBr. Lercher and co-workers found that $LaCl_3$ was a superior catalyst for this reaction, which provided CH_3Cl with a selectivity of around 55% at a CH_4 conversion of 12% at 748 K.[8]

Herein, we present a novel catalytic route for the conversion of CH_4 to propylene via monohalogenomethane. Propylene is one of the most important bulk chemicals, and currently, it is mainly produced as a coproduct of ethylene through the cracking of naphtha. However, the demand for propylene is growing much faster than the demand for ethylene.[9] The development of novel routes for the production of propylene, for example, dehydrogenation of propane,[9] conversion of methanol to propylene,[10] and conversion of ethylene to propylene,[11] has attracted much attention. Our two-step route from CH_4 to propylene can be expressed by Equations (1) and (2). Both reactions are exothermic (see the Supporting Information for details). The net reaction is the oxidation of CH_4 by O_2 to propylene and H_2O [Eq. (3)]. The development of efficient catalysts for the two reaction steps is the key to this new route.

$$CH_4 + HCl\ (HBr) + 1/2\ O_2 \xrightarrow{\text{catalyst A}} CH_3Cl\ (CH_3Br) + H_2O \quad (1)$$

$$CH_3Cl\ (CH_3Br) \xrightarrow{\text{catalyst B}} 1/3\ C_3H_6 + HCl\ (HBr) \quad (2)$$

$$\text{Net:}\quad CH_4 + 1/2\ O_2 \longrightarrow 1/3\ C_3H_6 + H_2O \quad (3)$$

We have investigated the catalytic performances of a variety of non-noble metal catalysts for the oxidative chlorination and bromination of CH_4. Among various metal oxides, CeO_2 is the most efficient catalyst for both reactions (see Tables S1 and S2 in the Supporting Information). CeO_2 was a particularly good catalyst for the oxidative chlorination of CH_4; a CH_3Cl selectivity of 66% and a CH_4 conversion of 12% were attained at 753 K. A higher temperature was required to obtain a similar CH_4 conversion by the oxidative bromination of CH_4; CH_4 conversion and CH_3Br selectivity were 16% and 74%, respectively, with CeO_2 at 833 K. Besides CH_3Cl and CH_3Br, CH_2Cl_2 and CH_2Br_2 were also formed in both reactions, but their selectivities were lower. $CHCl_3$ or $CHBr_3$ and CCl_4 or CBr_4 were not formed. The product distribution for the oxidative chlorination of CH_4 over CeO_2 is very different from that observed for the radical

[*] J. He,[+] T. Xu,[+] Z. Wang, Prof. Dr. Q. Zhang, Dr. W. Deng, Prof. Dr. Y. Wang
State Key Laboratory of Physical Chemistry of Solid Surfaces and National Engineering Laboratory for Green Chemical Productions of Alcohols, Ethers, and Esters
College of Chemistry and Chemical Engineering
Xiamen University, Xiamen 361005 (China)
E-mail: zhangqh@xmu.edu.cn
wangye@xmu.edu.cn

[+] These authors contributed equally to this work.

[**] This work was supported by the National Basic Research Program of China (2010CB732303) and the NSF of China (21033006, 20873110, and 20923004).

Supporting information for this article is available on the WWW under http://dx.doi.org/10.1002/anie.201104071.

reaction of CH_4/Cl_2, the main products of which were CH_2Cl_2 and $CHCl_3$.[2]

Recent studies have shown that the redox and catalytic properties of CeO_2 may be dependent on morphologies.[12] Understanding the effect of morphologies or exposed crystal planes of well-defined CeO_2 nanocrystals may provide an opportunity to unravel the nature of active structures, and is helpful for the rational design of more efficient catalysts. We have studied the effect of the morphology of CeO_2 on its catalytic behaviors in the oxidative chlorination and bromination of CH_4. We synthesized CeO_2 nanocrystals with the same cubic fluorite phase but different morphologies (nanorod, nanocube, and nano-octahedron) by hydrolysis of cerium(III) salts combined with a hydrothermal treatment.[12b] Measurements by transmission electron microscopy (TEM) and scanning electron microscopy (SEM) showed the uniform morphology of our synthesized CeO_2 nanocrystals (Supporting Information, Figure S1). The sizes of the nanorods, nanocubes, and nano-octahedra were $(9\pm4)\times(60$–$300)$ nm, 10–80 nm, and 100–200 nm, respectively. Their specific surface areas measured by N_2 adsorption at 77 K were 99, 23, and 21 m^2g^{-1}, respectively. High-resolution TEM (HRTEM) images showed that the nanorods exposed the {110} and {100} planes with fractions of 51% and 49%, respectively, while the nanocubes and the nano-octahedra exposed the {100} and {111} planes with nearly 100%, respectively (Supporting Information, Figure S2). For comparison, CeO_2 nanoparticles with a mean diameter of approximately 9 nm and a surface area of 146 m^2g^{-1} were also synthesized, and HRTEM images showed that the CeO_2 nanoparticles mainly exposed {111} planes (Supporting Information, Figure S3).

We confirmed that the morphologies of the CeO_2 nanocrystals were sustained after the oxidative chlorination and bromination of CH_4, although their sizes changed, particularly the length of the nanorods and the size of the nanoparticles (Supporting Information, Figure S3C and Figure S4). We have compared the intrinsic rates of CH_4 conversion ($r(CH_4)$) and product formation ($r(CH_3Cl)$ or $r(CH_3Br)$), that is, the amounts of converted CH_4 and formed product at controlled CH_4 conversions per surface area per time unit, among the CeO_2 catalysts with different morphologies (see Figure S5 in the Supporting Information for the calculation of intrinsic rates). The CeO_2 nanorods show the highest $r(CH_4)$ and $r(CH_3Cl)$ for the oxidative chlorination of CH_4, followed by nanocubes, nano-octahedra, and nanoparticles (Table 1). For the oxidative bromination of CH_4, the nanorods and nanocubes possess similar $r(CH_4)$ and $r(CH_3Br)$, which are higher than the nano-octahedra and nanoparticles. These results suggest that in both reactions the {100} and {110} planes of CeO_2 are more active than the {111} plane.

For the selective oxidation of CH_4 to HCHO by O_2 over most heterogeneous catalysts, the HCHO selectivity decreased sharply with increasing CH_4 conversion, thus leading to very limited HCHO yields (<5%).[1b,c,h] For the oxidative chlorination or bromination of CH_4 over CeO_2 nanocrystals, CH_3Cl or CH_3Br selectivities decreased only modestly with increasing CH_4 conversion by increasing the amount of catalyst (Figure 1). Moreover, CH_3Cl or CH_3Br selectivity depended on the morphology of CeO_2. The nanocubes, which exposed {100} planes, were the most selective catalysts, while the nano-octahedra and nanoparticles exposing mainly {111} planes were the least selective for the CH_3Cl or CH_3Br formation.

We performed in situ Raman spectroscopic studies for CeO_2 catalysts under the reaction conditions. Only Raman bands ascribed to CeO_2 were observed, and no $CeCl_3$ or

Table 1: Rates of methane conversion and product formation over CeO_2 nanocrystals with different morphologies and nanoparticles.[a]

Catalyst	Exposed planes	Surface area[b] [m^2g^{-1}]	$r(CH_4)$ [$mmol\,m^{-2}h^{-1}$]	$r(CH_3X)$ [$mmol\,m^{-2}h^{-1}$]
A) Oxidative chlorination				
Nanorod	{100} + {110}	54	0.93	0.64
Nanocube	{100}	20	0.72	0.54
Nano-octahedron	{111}	19	0.69	0.45
Nanoparticle	{111}	68	0.57	0.38
B) Oxidative bromination				
Nanorod	{100} + {110}	52	0.63	0.42
Nanocube	{100}	18	0.62	0.47
Nano-octahedron	{111}	10	0.54	0.38
Nanoparticle	{111}	64	0.50	0.32

[a] Reaction conditions: A) $T=753$ K, $CH_4/HCl/O_2/N_2/He=4/2/1/1.5/1.5$, total flow rate = 40 $mL\,min^{-1}$; B) $T=873$ K, 40 wt% HBr aqueous solution 4.0 $mL\,h^{-1}$, $CH_4/O_2/N_2=4/1/1$ (flow rate = 15 $mL\,min^{-1}$). [b] The specific surface areas listed here are those measured for the used catalysts. X = Cl, Br.

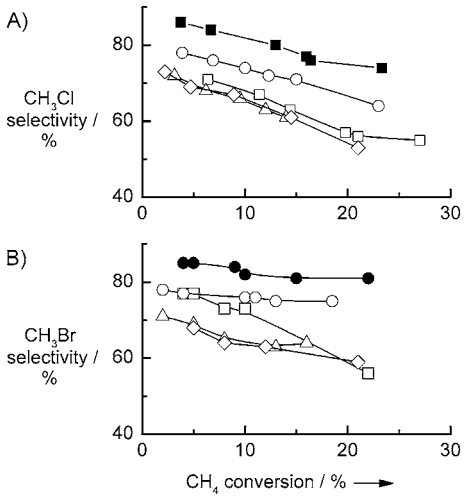

Figure 1. Selectivities of CH_3Cl (A) and CH_3Br (B) formations versus CH_4 conversions in the oxidative chlorination and bromination of CH_4 over CeO_2 nanocrystals with different morphologies and the modified CeO_2 nanocrystals. Reaction conditions: A) $T=753$ K, $CH_4/HCl/O_2/N_2/He=4/2/1/1.5/1.5$, total flow rate = 40 $mL\,min^{-1}$; B) $T=873$ K, 40 wt% HBr aqueous solution 4.0 $mL\,h^{-1}$, $CH_4/O_2/N_2=4/1/1$ (flow rate = 15 $mL\,min^{-1}$). ● NiO–CeO_2 cube, ■ FeO_x–CeO_2 rod, ○ cube, □ rod, △ octahedron, ◇ particle.

CeOCl was formed under the reaction conditions (see Figure S6 in the Supporting Information for the results of CeO_2 nanocubes). This suggests that CeO_2 is the active phase. Concerning the nature of the structure sensitivity (different catalytic behaviors of different exposed planes), theoretical studies showed that the {111} plane of CeO_2 has the lowest surface energy, followed by the {110} and {100} planes.[13] CeO_2 nanoparticles, which mainly expose {111} planes, show lower CO oxidation activity than CeO_2 nanorods and nanocubes.[12] Our H_2-TPR (temperature-programmed reduction) studies showed that the reduction of Ce^{4+} to Ce^{3+} was easiest for the nanorods, followed by the nanocubes, nano-octahedra, and nanoparticles (Supporting Information, Figure S7). This is in agreement with the CH_4 conversion rates for CeO_2 catalysts with different morphologies. We have proposed a possible reaction mechanism for the oxidative chlorination and bromination of CH_4 over CeO_2 catalysts (Supporting Information, Figure S8). We suggest that the reduction of Ce^{4+} to Ce^{3+} plays a key role in the activation of HCl or HBr to form an active Cl or Br species for CH_4 conversion, and the reduced Ce^{3+} is reoxidized to Ce^{4+} by O_2.

We have examined the effect of various additives on the catalytic performances of CeO_2 nanocrystals, and found that, compared to single CeO_2 nanorod or nanocube, the 15 wt% FeO_x–CeO_2 nanorod and the 10 wt% NiO_x–CeO_2 nanocube provided improved performances, especially selectivities; CH_3Cl and CH_3Br selectivities of 74% and 82% were attained at CH_4 conversions of 23% and 22%, respectively (Figure 1). Solid-solution phases were formed between FeO_x or NiO with CeO_2 in the composites, and the heteroatoms in CeO_2 might promote the adsorption and activation of HCl or HBr to form active Cl or Br species (Supporting Information, Figure S8). The FeO_x–CeO_2 nanorod and NiO_x–CeO_2 nanocube catalysts were stable during the oxidative chlorination and bromination of CH_4. During these reactions, the selectivities of CH_3Cl and CH_3Br stayed almost unchanged over approximately 100 hours, and CH_3Cl and CH_3Br could be sustained in more than 15% yields over these catalysts (Figure 2).

For the second step, that is, the conversion of CH_3Cl or CH_3Br to olefins, only few studies have been reported. A few research groups showed that zeolite SAPO-34 could catalyze the formation of lower olefins from CH_3Cl and CH_3Br, but the selectivity of the formation of C_2H_4 was higher than that of C_3H_6, which was on the level of 20–40%.[14–16] SAPO-34 underwent quick deactivation in a few hours in these reactions. Li^+-exchanged ZSM-5 could catalyze the CH_3Cl conversion, but the C_3H_6 selectivity was also low.[17] We first compared the catalytic performances of several H-form zeolites for the conversion of CH_3Br, and found that H-ZSM-5 exhibited a markedly higher CH_3Br conversion and a moderate C_3H_6 selectivity (Supporting Information, Table S3).

We have succeeded in improving C_3H_6 selectivity by treating H-ZSM-5 with an aqueous solution of NH_4F followed by calcination. By increasing the concentration of NH_4F (expressed as the molar ratio of F/Si) used for H-ZSM-5 treatment, C_3H_6 selectivity increased significantly for both CH_3Br and CH_3Cl conversions (Table 2). At the same time,

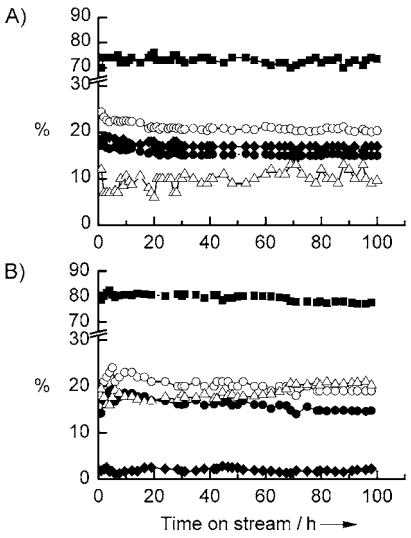

Figure 2. Dependences of catalytic performances on time on stream for the oxidative chlorination of CH_4 over the 15 wt% FeO_x–CeO_2 nanorods (A) and the oxidative bromination of CH_4 over the 10 wt% NiO–CeO_2 nanocubes (B). Reaction conditions: A) catalyst (0.50 g), $T = 753$ K, $CH_4/HCl/O_2/N_2/He = 4/2/1/1.5/1.5$, total flow rate = 40 mL min^{-1}; B) catalyst (1.0 g), $T = 873$ K, 40 wt% HBr aqueous solution 4.0 mL h^{-1}, $CH_4/O_2/N_2 = 4/1/1$ (flow rate = 15 mL min^{-1}). ■ CH_3X selectivity, ○ CH_4 conversion, ● CH_3X yield, △ CO_x selectivity, ◆ CH_2X_2 selectivity. X = Cl (A), X = Br (B).

the selectivities of the formation of C_2–C_4 alkanes and C_2H_4 decreased correspondingly. Besides the products listed in Table 2, C_x hydrocarbons ($x \geq 5$), particularly aromatic compounds, were also formed and the selectivity of their formation decreased when the F/Si ratio was increased. While an F/Si ratio that was too high was disadvantageous to the conversion of CH_3Br or CH_3Cl, the decrease in the activity was insignificant at proper F/Si ratios. The F-modified

Table 2: Effect of modification of H-ZSM-5 by NH_4F for the conversions of CH_3Br and CH_3Cl.[a]

F/Si ratio	Conv. [%]	Selectivity[b] [%] CH_4	$C_{2-4}{}^{0}$[c]	C_2H_4	C_3H_6	C_4H_8	Yield of C_3H_6 [%]
A) CH_3Br conversion							
0	92	1.2	23	13	30	13	28
0.031	98	0.9	11	11	38	20	38
0.047	98	1.0	5.0	7.5	46	25	45
0.063	94	1.4	1.5	4.3	56	23	53
0.079	87	1.5	0.4	3.1	59	25	51
0.095	35	3.5	0	1.8	63	30	23
B) CH_3Cl conversion							
0	88	1.6	37	18	18	5.8	16
0.031	83	1.9	26	20	27	9.9	22
0.047	89	1.0	8.1	12	46	20	41
0.063	76	1.3	1.1	4.8	64	23	49
0.079	68	1.4	0.6	3.5	67	23	45
0.095	55	1.3	0.5	3.0	67	26	37

[a] Reaction conditions: A) catalyst (0.10 g), $T = 673$ K, $P(CH_3Br) = 9.2$ kPa, flow rate = 11 mL min^{-1}, time on stream = 2 h; B) catalyst (0.30 g), $T = 673$ K, $P(CH_3Cl) = 3.3$ kPa, flow rate = 15 mL min^{-1}, time on stream = 2 h. [b] The remaining products were C_x hydrocarbons ($x \geq 5$). [c] C_2–C_4 alkanes.

H-ZSM-5 with an F/Si ratio of 0.063 afforded the best C_3H_6-formation activity in both CH_3Br and CH_3Cl conversions; C_3H_6 selectivities of 56% and 64% were attained at CH_3Br and CH_3Cl conversions of 94% and 76%, respectively. To the best of our knowledge, these superior C_3H_6 formation performances have to date never been achieved in the conversions of halogenomethanes.

The rapid deactivation was a serious problem for zeolite-catalyzed CH_3Cl and CH_3Br conversions.[14–17] Our results revealed that H-ZSM-5 was also deactivated seriously in CH_3Cl conversion (Supporting Information, Figure S9). However, the modification by fluorine significantly improved the stability of the catalyst. With the F-modified H-ZSM-5 (F/Si = 0.063), C_3H_6 selectivity kept almost unchanged, and CH_3Cl conversion decreased only slightly within 50 hours (Figure 3A). Moreover, the regeneration of the catalyst was possible by a simple treatment in air at the reaction temperature for two hours. The F-modified H-ZSM-5 was also stable in the conversion of CH_3Br to C_3H_6 (Figure 3B).

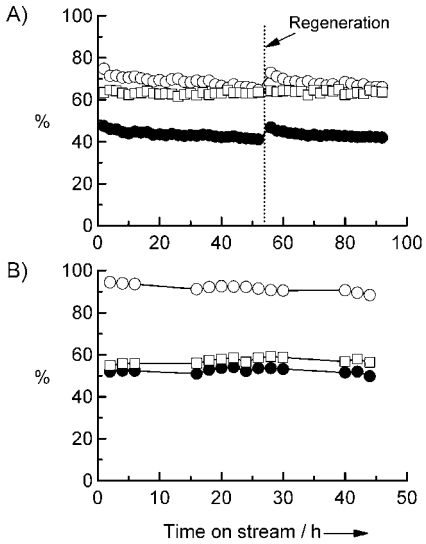

Figure 3. Catalytic performances of F-modified H-ZSM-5 versus time on stream for the conversions of CH_3Cl (A) and CH_3Br (B). Reaction conditions: A) catalyst (0.30 g), $T = 673$ K, $P(CH_3Cl) = 3.3$ kPa, flow rate = 15 mL min^{-1}; B) catalyst (0.10 g), $T = 673$ K, $P(CH_3Br) = 9.2$ kPa, flow rate = 11 mL min^{-1}. ○ CH_3X conversion, □ C_3H_6 selectivity, ● C_3H_6 yield. X = Cl (A), X = Br (B)

We have characterized the F-modified H-ZSM-5 to gain insights into the nature of F modification. Powder X-ray diffraction (XRD) measurements showed that the modification did not significantly change the crystalline structure of ZSM-5 (Supporting Information, Figure S10). However, the acidity and porous structure of ZSM-5 underwent significant changes after modification. The concentration of the acid sites, particularly the strong Brønsted acid sites, was dramatically decreased after F modification (Supporting Information, Figure S11). The same phenomenon was also observed previously and was proposed to contribute to the inhibition of catalyst deactivation in the dehydro-aromatization of CH_4 to benzene.[18] The weakened acidity may also be beneficial to catalyst stability in our case. Moreover, the decrease in the strong Brønsted acidity may suppress the hydrogen transfer and the aromatization reactions,[19] and thus contribute to the increase in C_3H_6 selectivity by inhibiting the formations of lower alkanes and aromatic compounds (Table 2).

We found that, in addition to the micropores with sizes of 0.51–0.55 nm, which is typical for ZSM-5, new micropores with sizes of 0.73–0.78 nm were generated after F modification (Supporting Information, Figure S12). The generation of the larger micropores was confirmed by the adsorption studies with *p*-xylene and *o*-xylene (Supporting Information, Table S4). This may be due to the F-induced desilication in peculiar positions of ZSM-5.[20] We speculate that the interaction of the F^- anions with the nearby framework Si may produce SiF_4 gas, particularly at the calcination stage, thus creating larger micropores (Supporting Information, Figure S13).

For the formation of lower olefins from both CH_3OH and CH_3Cl the "hydrocarbon pool" mechanism has been proposed, in which the lower olefins are believed to be generated via methylbenzene intermediates.[10b,21] We have characterized the hydrocarbon intermediates with our catalysts by a method reported previously,[22] and observed various methylbenzenes over H-ZSM-5 and F-modified H-ZSM-5 (Supporting Information, Table S5). It is of significance that the distribution of methylbenzenes is different over the two catalysts, and the modification by F increased the fraction of tetra-, penta-, and hexa-benzenes, which are proposed mainly for C_3H_6 formation.[22] The generated larger micropores in the F-modified H-ZSM-5 may account for this change in the distribution of the intermediates in the hydrocarbon pool on catalyst surfaces. Based on these results, we have proposed reaction mechanisms for the conversions of CH_3Cl or CH_3Br over H-ZSM-5 and F-modified H-ZSM-5 catalysts (Supporting Information, Figure S14).

In conclusion, we have developed novel and efficient catalysts for a new two-step route for the production of propylene from methane via CH_3Cl or CH_3Br. CeO_2 is an efficient and stable catalyst for the oxidative chlorination and bromination of methane to CH_3Cl and CH_3Br. The catalytic properties of CeO_2 are dependent on its morphology or the exposed crystalline planes. The modification of CeO_2 nanocrystals by FeO_x or NiO could enhance the selectivity of CH_3Cl or CH_3Br formation. For the second step, an F-modified H-ZSM-5 is highly selective and stable for the conversions of both CH_3Cl and CH_3Br into propylene.

It is noteworthy that Periana et al.[23] once developed an efficient two-step conversion of methane to methanol via methyl bisulfate by using oleum as an oxidant. However, this system suffers from the difficulties in the separations of product and catalyst from the oleum medium and in the recovery and reoxidation of the produced SO_2. In contrast, the product can be easily separated from our heterogeneous catalytic system. Although HCl and HBr are not particularly environmentally friendly, the easy separation and recycling of HCl or HBr in our case could avoid their net release. The overall efficiencies for HCl and HBr were estimated to be 65–70% and 90–93%, respectively, without considering the uses of CH_2Cl_2 and CH_2Br_2 formed in the first step (see Supporting Information for details). Future studies are needed to further

improve the selectivity of target products and to elucidate the detailed reaction mechanism for each step.

Experimental Section

CeO_2 nanocrystals with different morphologies as well as CeO_2 nanoparticles with a large surface area were synthesized by hydrolysis of $Ce(NO_3)_3$ in alkaline medium, followed by hydrothermal treatment.[12b] The morphologies were controlled by varying the alkaline media, $Ce(NO_3)_3$ concentrations, and the hydrothermal conditions. The FeO_x–CeO_2 nanorods and NiO_x–CeO_2 nanocubes were prepared by adding $Fe(NO_3)_3$ and $NiCl_2$ into aqueous solutions of $Ce(NO_3)_3$, followed by hydrolysis and hydrothermal treatment procedures used for syntheses of CeO_2 nanorods and nanocubes, respectively. H-ZSM-5 (Si/Al = 100) was used for CH_3Cl and CH_3Br conversions. The F-modified H-ZSM-5 was prepared by treating the H-ZSM-5 with aqueous solutions of NH_4F in different concentrations. After drying at 343 K, the samples were calcined at 873 K for 6 h. XRD, N_2 or Ar physisorption, SEM, TEM, NH_3-TPD (temperature-programmed desorption), H_2-TPR, and in situ Raman spectroscopy were used for catalyst characterizations. Catalytic reactions were performed on fixed-bed flow reactors operated under atmospheric pressure. The products were analyzed by gas chromatography. The conversion and selectivity for each reaction were calculated on a carbon basis. See the Supporting Information for the experimental details.

Received: June 14, 2011
Revised: January 2, 2012
Published online: January 24, 2012

Keywords: cerium oxide · heterogeneous catalysis · methane · propylene · zeolites

[1] a) D. Wolf, *Angew. Chem.* **1998**, *110*, 3545 – 3547; *Angew. Chem. Int. Ed.* **1998**, *37*, 3351 – 3353; b) K. Tabata, Y. Teng, T. Takemoto, E. Suzuki, M. A. Bañares, M. A. Peña, J. L. G. Fierro, *Catal. Rev.* **2002**, *44*, 1 – 58; c) A. Arena, A. Parmalina, *Acc. Chem. Res.* **2003**, *36*, 867 – 875; d) Y. Xu, X. Bao, L. Lin, *J. Catal.* **2003**, *216*, 386 – 395; e) R. Palkovits, M. Antonietti, P. Kuhn, A. Thomas, F. Schüth, *Angew. Chem.* **2009**, *121*, 7042 – 7045; *Angew. Chem. Int. Ed.* **2009**, *48*, 6909 – 6912; f) B. Frank, J. Zhang, R. Blume, R. Schögl, D. S. Su, *Angew. Chem.* **2009**, *121*, 7046 – 7051; *Angew. Chem. Int. Ed.* **2009**, *48*, 6913 – 6917; g) C. Copéret, *Chem. Rev.* **2010**, *110*, 656 – 680; h) Q. Zhang, W. Deng, Y. Wang, *Chem. Commun.* **2011**, *47*, 9275 – 9292; i) H. Schwarz, *Angew. Chem.* **2011**, *123*, 10276 – 10297; *Angew. Chem. Int. Ed.* **2011**, *50*, 10096 – 10115.

[2] G. A. Olah, B. Gupta, M. Farina, J. D. Felberg, W. M. Ip, A. Husain, R. Karpeles, K. Lammertsma, A. K. Melhotra, N. J. Trivedi, *J. Am. Chem. Soc.* **1985**, *107*, 7097 – 7105.

[3] X. P. Zhou, A. Yilmaz, G. A. Yilmaz, I. M. Lorkovic, L. E. Laverman, M. Weiss, J. H. Sherman, E. W. McFarland, G. D. Stucky, P. C. Ford, *Chem. Commun.* **2003**, 2294 – 2295.

[4] http://www.grt-inc.com/go/technology/grt-technology/.

[5] a) K. X. Wang, H. F. Xu, W. S. Li, X. P. Zhou, *J. Mol. Catal. A* **2005**, *225*, 65 – 69; b) Z. Liu, L. Huang, W. S. Li, F. Yang, C. T. Au, X. P. Zhou, *J. Mol. Catal. A* **2007**, *273*, 14 – 20.

[6] F. Li, G. Yuan, *Angew. Chem.* **2006**, *118*, 6691 – 6694; *Angew. Chem. Int. Ed.* **2006**, *45*, 6541 – 6544.

[7] R. Lin, Y. Ding, L. Gong, W. Dong, J. Wang, T. Zhang, *J. Catal.* **2010**, *272*, 65 – 73.

[8] a) E. Peringer, S. G. Podkolzin, M. E. Jones, R. Olindo, J. A. Lercher, *Top. Catal.* **2006**, *38*, 211 – 220; b) S. G. Podkolzin, E. E. Stangland, M. E. Jones, E. Peringer, J. A. Lercher, *J. Am. Chem. Soc.* **2007**, *129*, 2569 – 2576; c) E. Peringer, M. Salzinger, M. Hutt, A. L. Lemonidou, J. A. Lercher, *Top. Catal.* **2009**, *52*, 1220 – 1231.

[9] A. H. Tullo, *Chem. Eng. News* **2003**, *81(50)*, 15 – 16.

[10] a) M. Stöcker, *Microporous Mesoporous Mater.* **1999**, *29*, 3 – 48; b) J. F. Haw, W. Song, D. M. Marcus, J. B. Nicholas, *Acc. Chem. Res.* **2003**, *36*, 317 – 326.

[11] a) H. Oikawa, Y. Shibata, K. Inazu, Y. Murai, S. Hyodo, G. Kobayashi, T. Baba, *Appl. Catal. A* **2006**, *312*, 181 – 185; b) M. Iwamoto, Y. Kousugi, *J. Phys. Chem. C* **2007**, *111*, 13 – 15; c) M. Taoufik, E. L. Roux, J. Thivolle-Cazat, J. M. Basset, *Angew. Chem.* **2007**, *119*, 7340 – 7343; *Angew. Chem. Int. Ed.* **2007**, *46*, 7202 – 7205; d) B. Lin, Q. Zhang, Y. Wang, *Ind. Eng. Chem. Res.* **2009**, *48*, 10788 – 10795.

[12] a) K. Zhou, X. Wang, X. Sun, Q. Peng, Y. Li, *J. Catal.* **2005**, *229*, 206 – 212; b) H. X. Mai, L. D. Sun, Y. W. Zhang, R. Si, W. Feng, H. P. Zhang, H. C. Liu, C. H. Yan, *J. Phys. Chem. C* **2005**, *109*, 24380 – 24385; c) N. Ta, M. Zhang, J. Li, H. Li, Y. Li, W. Shen, *Catal. Today* **2009**, *148*, 179 – 183.

[13] M. Nolan, S. Grigoleit, D. C. Sayle, S. C. Parker, G. W. Watson, *Surf. Sci.* **2005**, *576*, 217 – 229.

[14] Y. Wei, D. Zhang, Z. Liu, B. L. Su, *J. Catal.* **2006**, *238*, 46 – 57.

[15] S. Svelle, S. Aravinthan, M. Bjørgen, K. P. Lillerud, S. Kolboe, I. M. Dahl, U. Olsbye, *J. Catal.* **2006**, *241*, 243 – 254.

[16] A. Zhang, S. Sun, Z. J. A. Koman, N. Osterwalder, S. Gadewar, P. Stoimenov, D. J. Auerbach, G. D. Stucky, E. W. McFarland, *Phys. Chem. Chem. Phys.* **2011**, *13*, 2550 – 2555.

[17] D. Jaumain, B. L. Su, *J. Mol. Catal. A* **2003**, *197*, 263 – 273.

[18] Y. Li, L. Liu, X. Huang, X. Liu, W. Shen, Y. Xu, X. Bao, *Catal. Commun.* **2007**, *8*, 1567 – 1572.

[19] M. A. Sanchez-Castillo, R. J. Madon, J. A. Dumesic, *J. Phys. Chem. B* **2005**, *109*, 2164 – 2175.

[20] a) E. Aubert, F. Porcher, M. Souhassou, V. Petříček, C. Lecomte, *J. Phys. Chem. B* **2002**, *106*, 1110 – 1117; b) M. P. Attfield, C. R. A. Catlow, A. A. Sokol, *Chem. Mater.* **2001**, *13*, 4708 – 4713.

[21] Y. Wei, D. Zhang, F. Chang, Q. Xia, B. L. Su, Z. Liu, *Chem. Commun.* **2009**, 5999 – 6001.

[22] M. Bjørgen, F. Joensen, K. P. Lillerud, U. Olsbye, S. Svelle, *Catal. Today* **2009**, *142*, 90 – 97.

[23] a) R. A. Periana, D. J. Taube, E. R. Evitt, D. G. Loffer, P. R. Wentrcek, T. Masuda, *Science* **1993**, *259*, 340 – 343; b) R. A. Periana, D. J. Taube, S. Gamble, H. Taube, T. Satoh, H. Fujii, *Science* **1998**, *280*, 560 – 564.

